Macromolecules
ARTICLE

*Macromolecules* **2010**, *43*, 7713–7721 **7713**
DOI: 10.1021/ma1006792

# Supramolecular Assembly of Poly(styrene)-*b*-poly(4-vinylpyridine) and 1-Pyrenebutyric Acid in Thin Film and Their Use for Nanofabrication

**Biplab K. Kuila,* E. Bhoje Gowd,* and Manfred Stamm***

*Department of Nanostructured Materials, Leibniz Institute of Polymer Research Dresden, Hohe Strasse 6, D-01069 Dresden, Germany*

*Received March 29, 2010; Revised Manuscript Received May 10, 2010*

ABSTRACT: Supramolecular assembly (SMA) between poly(styrene)-*b*-poly(4-vinylpyridine) (PS-*b*-P4VP) and 1-pyrenebutyric acid (PBA) is investigated in thin films after annealing in a 1,4-dioxane atmosphere. The PBA selectively enriches with the P4VP block through hydrogen bonding between the carboxylic group of 1-pyrenebutyric acid and pyridine ring of P4VP. The supramolecular assembly of PS-*b*-P4VP with 1-pyrenebutyric acid resulted in changing the cylindrical morphology of pure block copolymer into lamellar morphology in thin film due to the increase of the block compositions of P4VP (PBA). Pure block copolymer after solvent annealing shows cylindrical microdomains normal to the substrate with a periodicity ~26 nm, whereas the SMA complex shows perpendicularly oriented lamella with a periodicity ~29 nm. These thin films were further immersed in ethanol, a good solvent for P4VP/P4VP (PBA) and a nonsolvent for PS to generate nanotemplates. These nanotemplates are effectively used for the fabrication of arrays of nanowires of different functional materials like metal or semiconductor.

## Introduction

Self-assembly of block copolymers (BCP) has received widespread attention in the nanoscience and nanotechnology research due to their tendency to form wide range of periodic structures in the nanoscopic length scale.[1−7] The size and shape of the periodic structures mainly depend on the number of copolymer blocks, their volume fraction, chain flexibility, chain architecture, and chemical interactions existing between the blocks. In most of the practical applications block copolymers are used in the form of thin films, and the structural behavior of BCP thin films compared with bulk materials is often much more complicated due to the interfacial interactions of the blocks with the underlying substrate, the surface energies of the blocks, and commensurability of the film thickness. Significant progress has been made in controlling the microdomain orientation and long-range order in BCP thin films.[5−10] This class of ordered materials are promising for applications[11−17] in many fields of nanoscience and nanotechnology such as surface patterning, lithography, and templating for the fabrication of ordered arrays of metal, magnetic, polymeric, and semiconducting nanomaterial of high density (terabits per $cm^2$) used for electronic, electrochemical, optoelectronic, magnetic, photonic, and biosensing device applications.

In recent years, it was demonstrated that a supramolecular approach to block copolymer self-assembly is a simple and powerful technique for fine-tuning of the block copolymer morphologies and has been successfully applied in bulk[18−21] and in thin films.[22−26] In this approach, a low molar mass additive is associated with one of the blocks by noncovalent interactions such as metal coordination, hydrogen bonding, van der Waals forces, $\pi-\pi$ interactions, and electrostatic effects.[20−32] These supramolecular assemblies (SMA) offer advantages over the covalently linked analogues, since different functionalities can be incorporated into the assemblies simply by substituting the small molecules. This will reduce the burden of synthesizing entirely new families of BCP. Another major advantage of SMA strategy is that the low molar mass additive can be removed easily from the SMA by selective dissolution to obtain a nanoporous material.[22,24] These nanopores and nanochannels that are lined with functional groups are readily available for further applications. Among various types of supramolecular assemblies, those containing hydrogen bonds hold a prominent place in supramolecular chemistry because of their directionality and versatility. The pioneering groups of Ikkala and ten Brinke have demonstrated the preparation of hierarchical polymeric materials through the complexation of 3-pentadecylphenol (PDP) and poly(styrene)-*block*-poly(4-vinylpyridine) (PS−P4VP) in bulk by hydrogen bonds.[18,33,34] The resultant complexes display a structure-within-structure pattern characterized by two length scales. Most of the studies using PDP as a low molar mass additive to form SMA with block copolymer have focused on the bulk, and recently, there are few reports on thin films of PS−P4VP (PDP)-based supramolecular assembly. These studies mainly focused on the morphology, phase behavior, and terrace formation of the SMA thin film.[23,25,26,35] ten Brinke et al.[23] showed the terrace formation of supramolecular thin films annealed under different chloroform vapor pressures. Very recently, Tung et al.[26] systematically studied PS-*b*-P4VP (PDP) with a wide range of P4VP-(PDP) weight fraction and established a correlation between orientation of supramolecular assembly in thin films and the weight fraction of P4VP (PDP). Also, they demonstrated the formation of hierarchical assemblies, e.g., lamellae-within-lamellae and cylinders-within-lamellae in thin films. A careful observation of AFM images reported on PS-*b*-P4VP (PDP) thin films indicated the huge surface roughness due to the unevenly distributed surfactant kind of additive (PDP) molecules over the thickness of the film. Our group has demonstrated the formation of smooth thin films from SMA of PS-*b*-P4VP and a nonsurfactant molecule having two different hydrogen-bonding groups 2-(4′-hydroxybenzeneazo)benzoic acid (HABA).[22,24] The orientation of the cylindrical microdomains P4VP (HABA) surrounded by PS

*To whom correspondence should be addressed. E-mail: biplab.kuila@yahoo.com, bhojegowd@yahoo.com and stamm@ipfdd.de.


Published on Web 08/19/2010

matrix could be switched by exposure to different solvent vapors. It is worth mentioning here that the uniform film formation and the homogeneous distribution of HABA molecules in SMA thin films are very sensitive to the film deposition conditions. We noticed that under some conditions HABA crystallized on the film surface upon drying of the film or solvent annealing of the film. It was noticed that if the interaction between block copolymer and small molecules is not strong enough to form comblike structure, additive will come out from the thin film and crystallize on the surface of the thin film during annealing and hampers the order and orientation of the microdomian.[36] Considering these difficulties, a limited number of reports are available on the study of block copolymer-based SMA in thin films, and in most of these studies PDP or HABA was used as a low molar mass additive to form the hydrogen bonding. It is necessary to add new additives to the library of PS-*b*-P4VP-based SMA for the complete understanding of constraints or factors which control the block copolymer supramolecular assembly and the orientation of the microdomain in thin film. There is also limited number of reports on complete transformation of the block copolymer morphology after supramolecular assembly with small molecules in thin film and their use as template for nanofabrication. In this article, we have studied the supramolecular assembly of a new molecule 1-pyrenebutyric acid with PS-*b*-P4VP. 1-Pyrenebutyric acid (PBA) is an important photoluminescence molecule used as fluorescent dye and electroluminescent dopant. PBA forms SMA with the P4VP block due to strong hydrogen bonding between the carboxylic group of 1-pyrenebutyric acid and pyridine ring of P4VP. The SMA of PS-*b*-P4VP with 1-pyrenebutyric acid resulted in changing of the cylindrical nanodomain of block copolymer into lamella in thin film due to compositional change. After fabricating the SMA thin film, the major component 1-pyrenebutyric acid can be easily removed by dissolving the thin film in ethanol to transform the block copolymer thin film into nanotemplate or membrane. We have also shown that these nanotemplates can be effectively used for the fabrication of arrays of nanowire of different functional material like metal or semiconductor. Such nanopatterned ultradense periodic arrays of metal or semiconductor nanoparticles may find potential applications in storage devices, photonic materials, and catalytic applications. We believe that our study on block copolymer-based supramolecular assembly in thin film and the nanofabrication using these nanotemplates is considered to make a significant contribution in the development of nanoscience and nanotechnology.

## Experimental Section

**Materials.** PS (32900)-*b*-P4VP (8000) (PDI = 1.06) was purchased from Polymer Source Inc. 1-Pyrenebutyric acid (PBA) (97%), cadmium acetate, thioacetamide, chloroauric acid ($HAuCl_4$), and sodium borohydride were purchased from Aldrich Sigma Chemicals. The solvents 1,4-dioxane, chloroform, tetrahydrofuran (THF), ethanol, and dichloromethane were purchased from Acros Organics and used as is. Silicon wafers {100} were cleaned successively in an ultrasonic bath (dichloromethane) for 15 min and a "piranha" bath (30% $H_2O_2$, 70% of $H_2SO_4$, *chemical hazard*) for 90 min at 75 °C and then thoroughly rinsed with Millipore water and dried under an argon flow. For the deposition of gold nanoparticle, the block copolymer thin film is deposited on glass substrate. The glass slides are cleaned by sonication in chloroform, ethanol, and water successively for 10 min in each solvent and finally dried by argon flow.

**Fabrication of Nanotemplate.** PS-*b*-P4VP and PBA (1 mol of PBA: 1 mol of 4-vinylpyridine monomer unit) were dissolved separately. PS-*b*-P4VP solution was then added drop-by-drop to PBA solution, while the solution was heated close to the boiling point of the solvent in an ultrasonic bath. The resulting solution (the total concentration PS-*b*-P4VP + PBA 1% (w/v)) was kept overnight to complete hydrogen-bonding formation. Thin films of PS-*b*-P4VP + PBA were prepared by the dip-coating method from the filtered composite solutions at rate of 1 mm $s^{-1}$. Dip-coated thin films were further annealed in saturated vapors of 1,4-dioxane for 4 days to improve the order of the nanodomains. Selective extraction of PBA from PS-*b*-P4VP + PBA thin film leads to the formation of block copolymer nanotemplate.

**Gold and Cadmium Sulfide Deposition on the Block Copolymer Nanotemplate.** The gold deposition was carried out similar to the reported method[37] with some modification. The polymer-coated glass substrate was immersed in the aqueous metal salt solution (consisting of 10 mL of 0.01 M $HAuCl_4$ and 10 mL of 0.01 M HCl) for 20 min. After metal salt deposition, the sample was thoroughly washed with water to remove the excess salt absorbed on the block copolymer template surface and dried under argon stream. Then the block copolymer template was dipped into freshly prepared sodium borohydride ($NaBH_4$) solution in water for the reduction of $HAuCl_4$, which was adsorbed onto the block copolymer nanotemplate. Formation of the gold nanostructures on glass was visually observed due to the color change. On the other hand, for CdS deposition, the block copolymer template on silicon substrate was dipped into 0.1 M cadmium acetate solution for 2 h. Then the silicon substrate containing block copolymer template was transferred from cadmium acetate solution to an aquas solution of thioacetamide, which acts as a source of sulfide ion ($S^{2-}$).

**Characterization of the Block Copolymer Thin Films.** *Thickness*. The thickness of the polymer films on silicon substrate was measured by an SE 400 ellipsometer (SENTECH Instruments GmbH, Germany) with a 632.8 nm laser at a 70° incident angle.

*FTIR*. Block copolymer thin films deposited on cleaned silicon wafers were directly used for FTIR measurements. Infrared spectra were recorded with a Bruker IFS 66v FTIR spectrometer in the reflectance mode.

*GISAXS*. GISAXS measurements were carried out at the beamline BW4 of the DORIS III storage ring at HASYLAB (DESY, Hamburg, Germany). The X-ray wavelength was $\lambda$ = 0.138 nm. The sample was placed horizontally on a goniometer. Two beam stops were used in these measurements. One beam stop was used to block the direct beam and a second one to block the very high specular intensity on the detector. The incident angle was set to $\alpha_i = 0.20°$, which is well above the critical angles of the polymer (0.16°) but below the critical angle for Si (0.22°). Therefore, the X-ray beam penetrates the whole film, and the scattering data give the information on the structural lengths present in the full depth of the film. The scattered intensities were recorded by a 2D detector (MARCCD; 2048 × 2048 pixel). Line-averaged intensities are reported as $I$ vs $q$, where $q = (4\pi/\lambda)\sin(\theta/2)$, $\lambda$ is the wavelength of incident X-rays, and $\theta$ is the scattering angle.

*AFM*. The AFM imaging was performed on as prepared samples on silicon or glass substrate by a Dimensions 3100 (NanoScope IV Controller) scanning force microscope in the tapping mode. The tip characteristics are as follows: spring constant 1.5−3.7 N $m^{-1}$, resonant frequency 45−65 kHz, tip radius about 10 nm.

*FESEM*. FESEM images were obtained with field emission electron microscopy (Zeiss Ultra 55 Gemini with FIB) operating at 3 kV. The samples were investigated without staining, and the working distance was 3 mm.

*UV−vis Study*. UV−vis study of the SMA template after gold deposition on glass substrate was done using a UV−vis spectrometer (Analytical Jena, Specord 40).

*Photoluminescence Study*. For the photoluminescence (PL) measurement, the thin films prepared from SMA after CdS deposition were dissolved in chloroform by sonication. The PL spectra of that solution were performed taking the solution in a

quartz cell of path length 1 cm in a Horiba Jobin Yvon (Fluoromax-3) luminescence spectrometer. The photoexcitation was made at an excitation wavelength of 320 nm.

## Results and Discussion

Block copolymer thin films based on supramolecular assembly of PS-*b*-P4VP and PBA were deposited on cleaned silicon wafer or glass substrate by dip-coating from 1% composite solution in 1,4-dioxane. Under an optical microscope, the polymer films with thicknesses about 30 nm are macroscopically and microscopically smooth and show no signs of PBA phase separation, such as crystals or stains. This suggests that PBA molecules are associated with P4VP blocks building comblike polymer chains. The chemical structure of the PS-*b*-P4VP (PBA) is shown in Figure 1a.

We have investigated the supramolecular assembly between PS-*b*-P4VP and PBA by FTIR. Figure 2 (Figure 2a from 1030 to 980 $cm^{-1}$ and Figure 2b from 1800 to 1620 $cm^{-1}$) shows the FT-IR spectra of PBA, PS-*b*-P4VP, and PS-*b*-P4VP (PBA) thin films before and after washing in ethanol. Free pyridine groups in the PS-*b*-P4VP thin film contribute to the absorption at 994 $cm^{-1}$ [19,20] (which is absent in PBA spectra). As seen from Figure 2a, the intensity of the absorption peak at 994 $cm^{-1}$ disappears in PS-*b*-P4VP (PBA) thin film and a new broad peak appears at 1014 $cm^{-1}$ which is due to the hydrogen-bonded pyridine ring,[19,20,26] which confirms the formation of supramolecular assembly between PS-*b*-P4VP and PBA through hydrogen bonding (see Figure 1a).

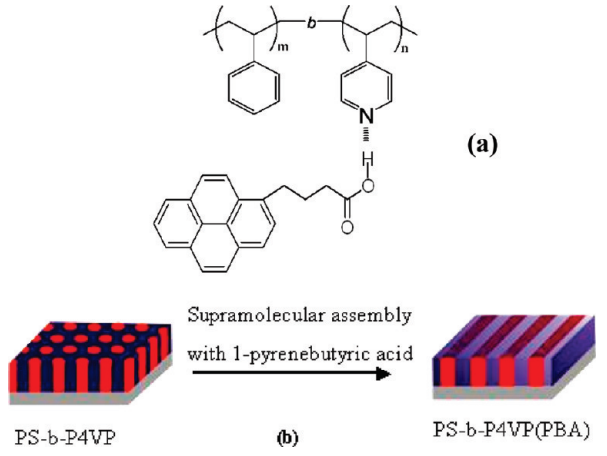


**Figure 1.** (a) Chemical drawing of the SMA formation through hydrogen bonding between P4VP block of PS-*b*-P4VP copolymer and PBA. (b) Schematic representation of transformation of the morphology of block copolymer thin film from cylindrical to lamella after the formation of supramolecular assembly.

The formation of hydrogen bonding is further confirmed by the band at 1695 $cm^{-1}$, which is corresponding to the stretching frequency of C=O bond from carboxylic acid group of PBA. As seen in Figure 2b, this band shifted to higher wavenumber at 1709 $cm^{-1}$ in PS−P4VP (PBA) due to hydrogen bonding between carboxylic group of PBA and pyridine ring of PS-*b*-P4VP. After immersing the PS-*b*-P4VP (PBA) thin film in ethanol, the free pyridine peaks are recovered, whereas the characteristic peaks of PBA have disappeared as shown in particular by the stretching frequency of C=O bond from carboxylic acid group of PBA at 1695 $cm^{-1}$. This indicates that washing with ethanol is an efficient way to eliminate PBA from the supramoleculear assembly to generate the nanotemplates.

The PS (32900)-*b*-P4VP (8000) (PDI = 1.06) block copolymer used here exhibits cylindrical morphology in bulk where the P4VP core is surrounded by PS matrix. Block copolymer thin films were prepared by the dip-coating process using 1% PS-*b*-P4VP solution in 1,4-dioxane. Figure 3 shows the atomic force microscope height images of the samples as dip-coated, solvent-annealed in 1,4-dioxane, and the corresponding structures after the surface reconstruction (rinsed with ethanol). The AFM images of as dip-coated film of pure block copolymer (Figure 3a) showed a disordered cylindrical microdomain due to fast solvent evaporation, leaving the chains insufficient time to rearrange to attain equilibrium morphology. 1,4-Dioxane vapor-annealed thin films assemble into hexagonally packed cylindrical microdomains oriented normal to the substrate (Figure 3b). When the solvent-annealed films were immersed into ethanol, a good solvent for P4VP and a nonsolvent for PS, a surface reconstruction of the films was observed with a fine structure (Figure 3c). Russell and co-workers have shown such a surface reconstruction process in PS-*b*-P4VP diblock copolymer thin films and demonstrated that the preferential solvation of P4VP blocks with ethanol does not alter the order or orientation of the microdomains.[38] Surface reconstruction of a 1,4-dioxane annealed film of pure block copolymer keeps the well-developed microdomain structure, having hexagonal order with an average center-to-center spacing of ≈26 nm and pore diameter of ≈12 nm (Figure 3c).

On the other hand, PBA added SMA thin film showed different morphology than the parent block copolymer thin film as shown in Figure 3d−f because of the selective interaction of PBA with P4VP blocks. The AFM image (Figure 3d) of the as dip-coated thin film of SMA shows no characteristic morphology. This morphology is kinetically trapped and far from the equilibrium due to the fast removal of the solvent during dip-coating.

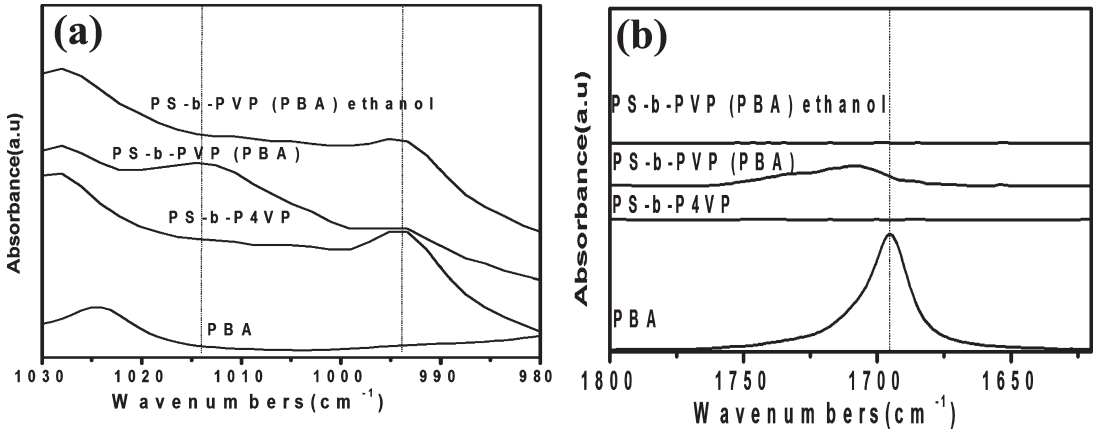


**Figure 2.** FT-IR spectra of PBA, PS-*b*-P4VP, PS-*b*-P4VP + PBA, and ethanol-washed PS-*b*-P4VP + PBA thin film in different regions: (a) 1030−980 $cm^{-1}$; (b) 1800−1620 $cm^{-1}$.

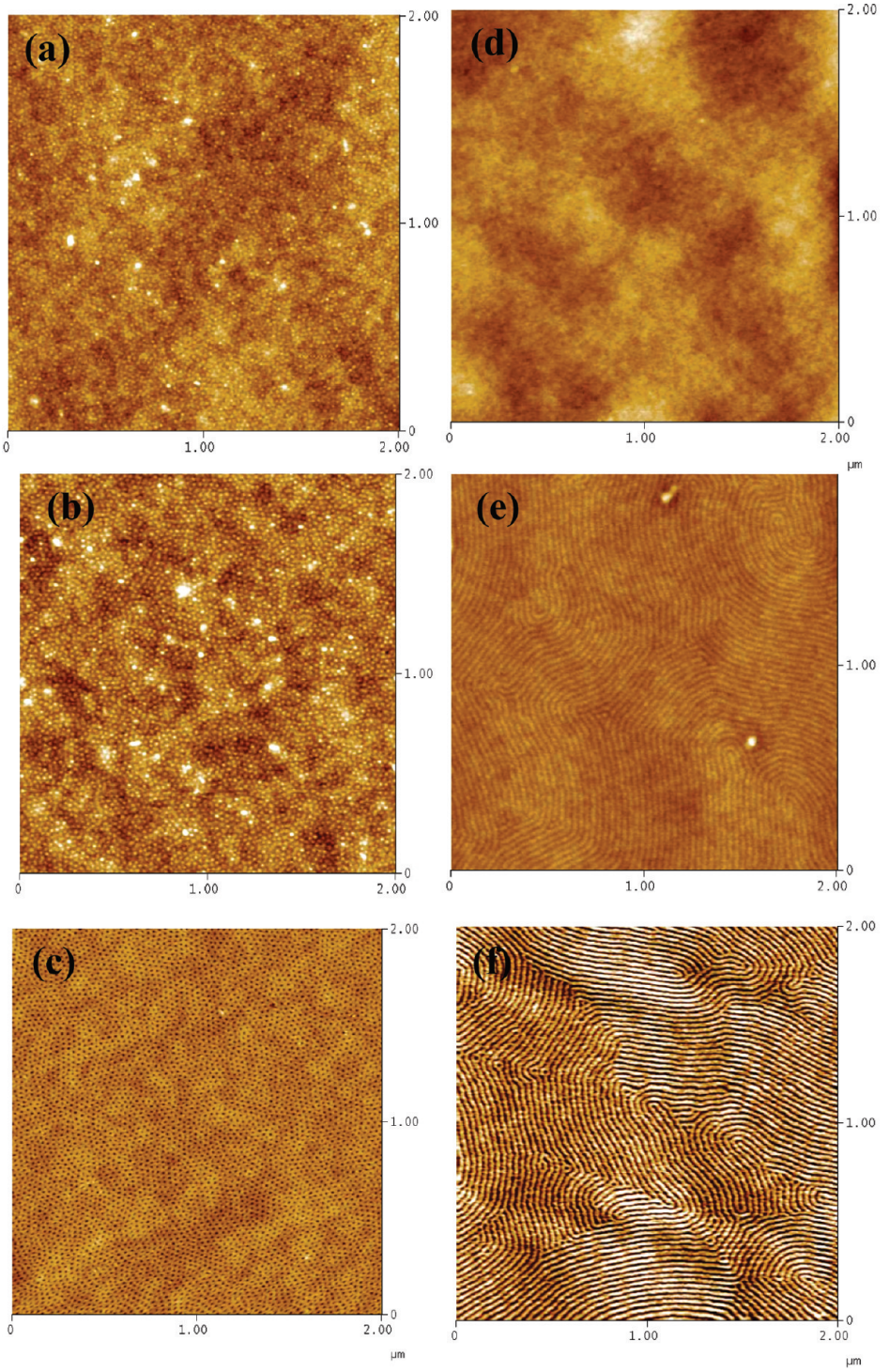


**Figure 3.** AFM height images of (a) PS-*b*-P4VP film as dip-coated from 1,4-dioxane solution, (b) 1,4-dioxane vapor-annealed block copolymer thin film, (c) 1,4-dioxane vapor-annealed block copolymer thin film after surface reconstruction, (d) thin film from SMA with PBA after dip-coating, (e) 1,4-dioxane vapor-annealed SMA thin film, and (f) 1,4-dioxane vapor-annealed SMA thin film after surface reconstruction.

On further annealing these SMA thin films in 1,4-dioxane vapors leads to the structural reorganization to lamellar structure, and the lamella are oriented normal to the substrate as shown Figure 3e. The surface reconstruction as well as the removal of PBA was done by dipping the SMA thin film in ethanol similar to the case of pure block copolymer. Figure 3f shows the AFM image of the SMA thin film on silicon substrate after surface reconstruction which demonstrates distinct lamella domain normal to the substrate (Figure 3f) with spacing of ≈29 nm. The complete removal of the PBA is also proved by the FTIR as discussed in the preceding section. In order to further confirm the morphology observed by AFM, we have also performed the FESEM study. Figure 4 shows the SEM images of nanotemplates from pure block copolymer and from supramolecular assembly after surface reconstruction. SEM results are in good correlation with the AFM results. Block copolymer nanotemplate shows hexagonally packed cylindrical channels perpendicular to the silicon substrate, whereas the SMA template reveals perpendicular lamellar structure.

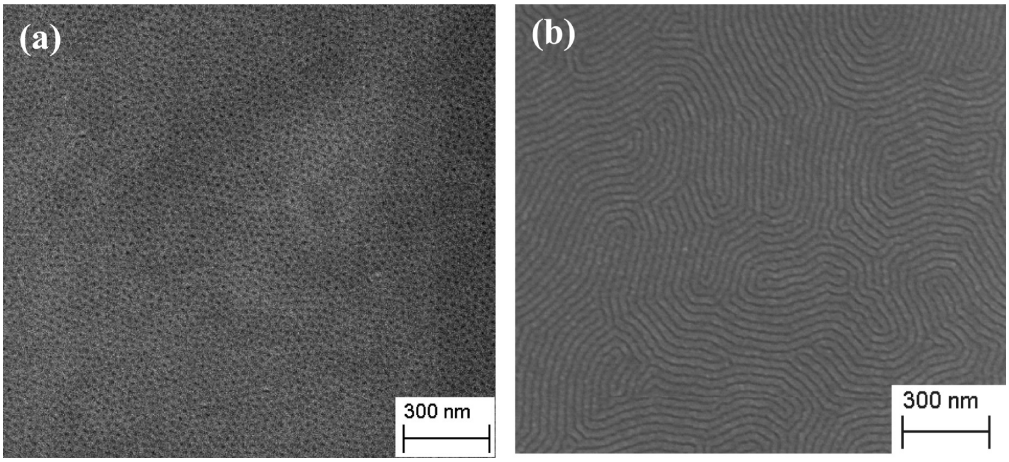


**Figure 4.** (a) Pure block copolymer thin film after surface reconstruction. (b) SMA thin film after surface reconstruction.

AFM and SEM give the surface morphology of the thin films; however, neither of these techniques allowed us to understand the buried structures inside the thin films. GISAXS is a powerful technique to investigate the internal morphology of thin films. Figure 5 shows the GISAXS patterns measured for various samples of PS-*b*-P4VP and PS-*b*-P4VP (PBA) thin films. The GISAXS 2D patterns are shown on the left side, whereas the in-plane profiles as a function $q_y$ are shown on the right side of each image. Figure 5A shows GISAXS 2D image along with the in-plane profile of 1,4-dioxane solvent-annealed block copolymer nanotemplate. The sharp Bragg rods (vertical streaks) in the GISAXS pattern correspond to the reflections from a 2D lattice of finite length oriented normal to the film surface. The reflections from the BC nanoporous thin film are located at the scattering vectors of $1{:}\sqrt{3}{:}\sqrt{4}$ relative to the first-order reflection, characteristic of hexagonally packed cylindrical microdomains. From the scattering vector of the primary reflection, the *d*-spacing was calculated to be 27 nm, which is consistent with the AFM and SEM observations. Figure 5B depicts the GISAXS images (2D and in-plane intensity profile) of as dip-coated SMA thin film from 1,4-dioxane solution. The absence of strong reflections, other than the primary reflection, indicates the lack of order in as dip-coated films. These films were further annealed in saturated vapors of 1,4-dioxane, and the PBA was removed by dipping the SMA thin film in ethanol for 20 min. Figure 5C shows the GISAXS 2D image along with the in-plane intensity profile of the SMA template. Similar to the BC nanoporous thin film, the extension of the scattering intensity along $q_z$ direction clearly indicates that the microstructures are oriented normal to the film surface. In this case, the reflections are located at the scattering vectors of 1:2:3 relative to the first-order reflection represent the lamellar microdomain morphology.

The first-order peak at $q_y = 0.218$ nm$^{-1}$ corresponds to a spacing of 29 nm, which is consistent with the AFM and SEM results. The preferential orientation of the microdomain normal to the substrate in block copolymer thin film or SMA thin film is also supported by other literature.[22,39] Sidorenko et al.[22] demonstrated the reversible switching phenomena in a supramolecular assembly based on PS-*b*-P4VP with HABA (2-(4′-hydroxybenzeneazo)benzoic acid) upon exposure to different solvent in thin film. This supramolecular assembly gives perpendicular cylinder annealed in 1,4-dioxane and reversibly switched to parallel cylinder upon exposure to chloroform. Recently, Gowd et al.[39] also observed the preferential orientation of the hexagonally arranged cylindrical microdomain in PS-*b*-P4VP block copolymer thin film annealed in 1,4-dioxane. In our case, we showed perpendicularly oriented lamellar microdomain of the SMA normal to the substrate in thin film upon solvent annealing in 1,4-dioxane. The preferential orientation of the microdomains can be attributed to the selectivity of the constituted blocks in that solvent[40] used for solution preparation and annealing. 1,4-Dioxane is a selective solvent for PS,[24] not for P4VP or P4VP (PBA) block. So annealing in 1,4-dioxane will induce the morphology consists of microdomains normal to the substrate. The morphology obtained upon evaporation of 1,4-dioxane is of course trapped in a nonequilibrium state. Heating the film above the glass transition temperature of the microdomain or annealing in a solvent which are almost equally selective for the both solvent will lead to the equilibrium state where microdomains are parallel to the surface.[24,41,42] Now it is important to discuss the reason for the change of the block copolymer thin film morphology after supramolecular assembly. The reason is obviously the composition change of the block copolymer film after the formation of supramolecular assembly. The PBA molecules are associated with P4VP blocks by hydrogen bonding and behave like comblike polymer chains as a whole. So the supramolecular assembly will effectively increase the block composition of P4VP due to the complexation with PBA through hydrogen bonding. Here, we used 1:1 molar ratio of P4VP and PBA for the formation of supramolecular assembly, and this ratio allowed us to estimate the molecular weight of the PBA associated P4VP chain after the formation of supramolecular assembly. Here, we assume that the assembly can be treated like a diblock copolymer. The phase behavior of diblock copolymers (A-*b*-B) is dictated by the Flory−Huggins segment−segment interaction parameter, $\chi$, the degree of polymerization, $N$, and the volume fraction of the blocks ($f_A$ and $f_B$). Matsen and Bates[43] demonstrate the phase diagram of block copolymer in between the weak ($\chi N \leq 10$) and strong ($\chi N \geq 10$) segregation regime. The diblock copolymer at $\chi N$ less than ca. 10.5 is always in disordered state disregarding the volume fraction of the blocks. From a random copolymer blend miscibility study, the $\chi$ value for the pure PS-*b*-P4VP diblock copolymer was determined to satisfy $0.30 < \chi_{PS-P4VP} \leq 0.35$ ($T \approx 160$ °C).[44,45] Very recently, a similar value of $0.317 < \chi_{PS-P4VP} \leq 0.347$ ($T$ between 160 and 195 °C) was found from a diblock copolymer scattering study.[46] Such a large value implies the strong segregation limit of PS-*b*-P4VP for moderate molecular weight. The pure block copolymer gives cylindrical morphology as equilibrium structure after microphase separation at room temperature. Now after formation of the SMA, the presence of PBA might effectively decreases the $\chi$ parameter between PS and P4VP, while $N$ stays constant; hence, the $\chi N$ value of the block copolymer will change accordingly but still remain in the strong segregation regime.

So the SMA should be in the ordered state at room temperature like the pure block copolymer. But the nature of the

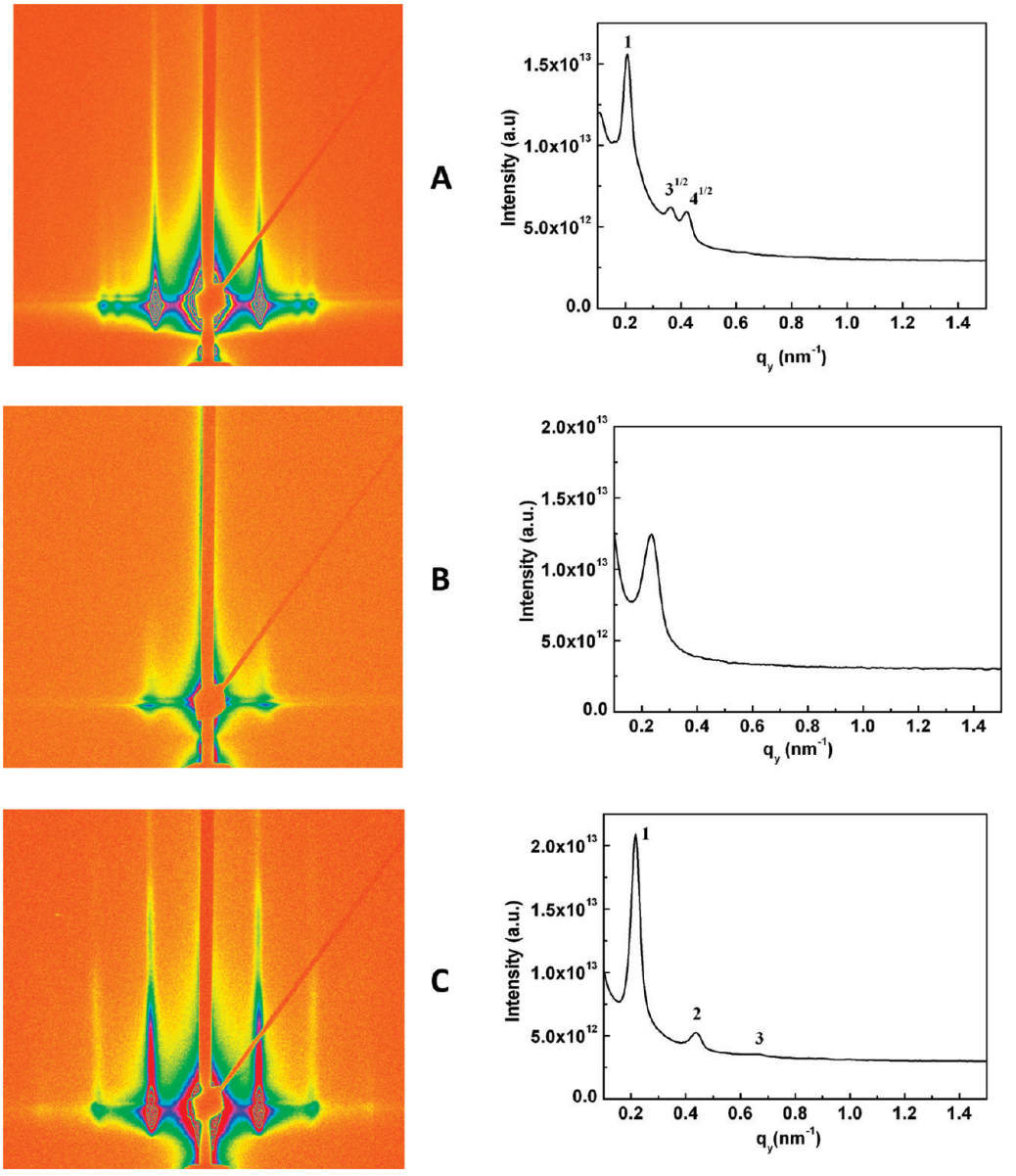


**Figure 5.** 2D GISAXS patterns and their corresponding in-plane intensity profiles. (A) Surface reconstructed PS-*b*-P4VP nanoporous template. (B) As dip-coated PS-*b*-P4VP (PBA) thin film. (C) 1,4-Dioxane annealed SMA template after the removal of PBA.

microphase separation is different, which results in a change in the morphology of the block copolymer after SMA due to the increase of volume fraction of the P4VP (PBA). The pure block copolymer initially shows cylindrical morphology that is transformed to lamellar morphology after forming SMA with PBA. The qualitative phase diagram is shown in Figure 6. Region 1 in the phase diagram denotes pure block copolymer ($f_{PS} \approx 0.804$) having hexagonally arranged cylindrical morphology. After the formation of SMA with PBA, the block copolymer ($f_{PS} \approx 0.476$) goes to region 2 in the phase diagram with lamellar morphology.

**Nanofabrication Using SMA-Based Templates.** SMA-based nanotemplates were generated by washing PBA from the PS-*b*-P4VP (PBA) SMA thin films. These templates were directly immersed into a mixture of $HAuCl_4$ and HCl. In the presence of HCl, the P4VP chains, which are available at the pore walls of the template, get protonated and readily bound to the anionic $AuCl_4^-$ through electrostatic interaction. The P4VP-decorated gold salt was further reduced to gold by sodium borohydride. Figure 7a shows SEM image of the SMA template after gold deposition, which corresponds to arrays of gold decorated lamella. After deposition of gold,

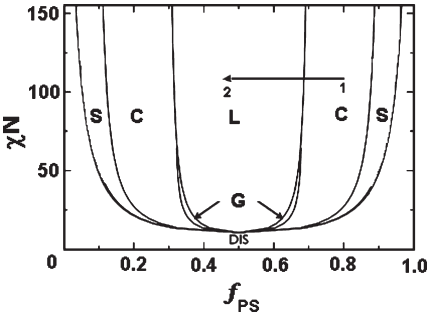


**Figure 6.** Qualitative phase diagram of the block copolymer (PS-*b*-P4VP) and their supramolecules based on Matsen and Bates phase diagram.[42] $f_{PS}$ is the block fraction of polystyrene block, $\chi$ is the Flory−Huggins interaction parameter, and $N$ is the length of the block. L = lamella, C = hexagonally packed cylinder, G = double gyroid, S = sphere. Region 1 denotes pure block copolymer having hexagonally packed cylinder, and region 2 denotes block copolymer-based supramolecules having lamellar structure.

the order and the spacing between the microdomains were still maintained as it was before. Figure 8a shows the AFM

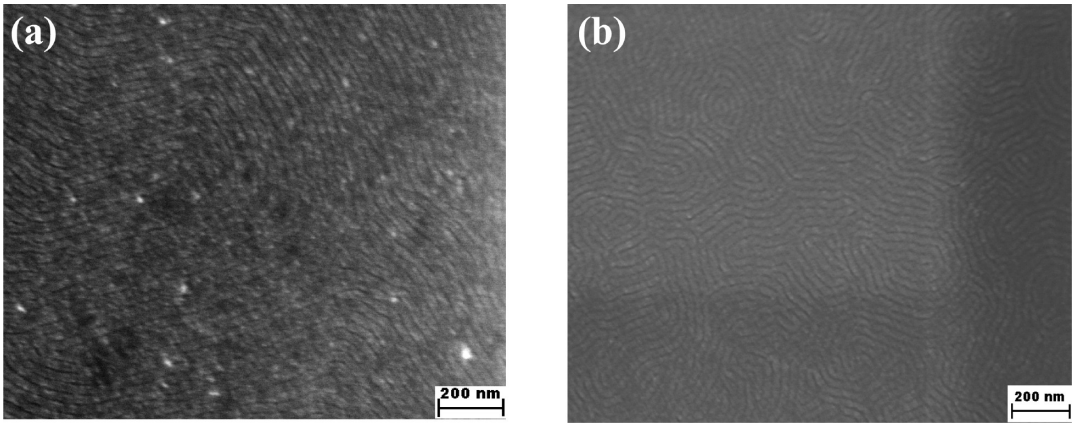


**Figure 7.** HRSEM images of SMA thin film after the deposition of (a) gold and (b) CdS.

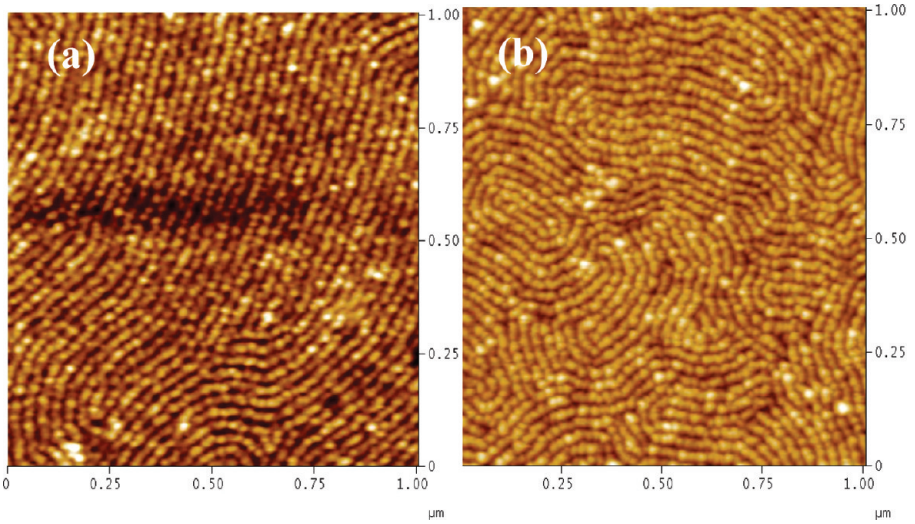


**Figure 8.** AFM images of SMA thin film after the deposition of (a) gold and (b) CdS.

image of the gold deposited block copolymer template, which clearly indicates that gold is deposited only on the P4VP domain of the lamella. The deposition of the block copolymer template is again confirmed by UV−vis study of the block copolymer thin film on glass substrate after gold deposition. Figure 9 shows the UV−vis spectra of gold deposited block copolymer template. The peak around 550 nm is due to the well-known plasmonic vibration band of gold nanoparticle.[47] We have also deposited semiconducting nanoparticles like CdS on these block copolymer templates. There are already few reports available in the literature on fabrication of arrays of CdS nanodots[48] by filling the block copolymer templates. But these methods involve some tedious and lengthy fabrication steps as well as it was difficult to fill the block copolymer templates uniformly. Here we delivered a novel method for uniform filling of the block copolymer template using cadmium sulfide as the precursor.

As mentioned in the preceding section, the SMA templates were directly dipped into aqueous solution of cadmium acetate for 4 h. The P4VP chains, which are at the pore walls of the templates, coordinate with $Cd^{2+}$ ion. These block copolymer templates coordinated with $Cd^{2+}$ ion are directly dipped into aquas solution of thioacetamide which acts as a source of $S^{2-}$ ion and produce cadmium sulfide nanoparticle stabilized by pyridine ring of P4VP chain. Excess of cadmium acetate molecules, which are loosely bound to the surface of SMA template, will go to thioacetamide solution.

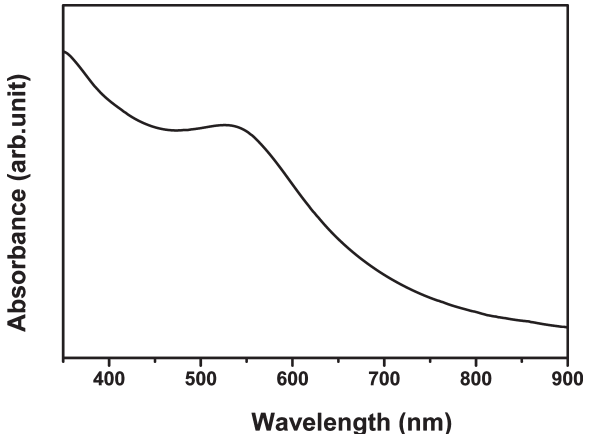


**Figure 9.** UV−vis spectra of gold deposited SMA template.

Figures 7b and 8b show the SEM and AFM images of the SMA template after CdS deposition, respectively. The deposition of CdS on the block copolymer lamella is more clearly visible in the AFM image rather than the SEM image. In order to confirm the deposition of CdS, we also performed the photoluminescence (PL) study. The CdS decorated SMA nanotemplates were dissolved in chloroform to study the PL. Figure 10 demonstrates the PL spectra of the solution of SMA template after CdS deposition. The peak at around

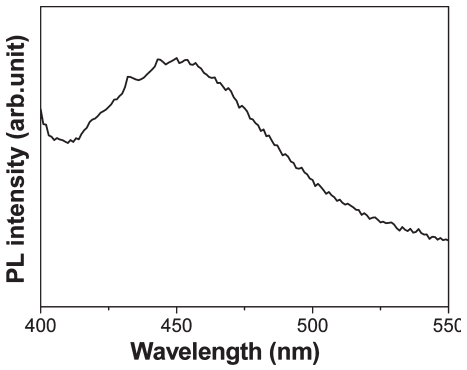


**Figure 10.** Photoluminescence study of thin film fabricated from SMA after CdS deposition. The excitation wavelength is 320 nm.

450 nm confirms the presence of CdS nanoparticles in the template.[49,50]

## Conclusion

In conclusion, we have described the supramolecular assembly between poly(styrene)-*b*-poly(4-vinylpyridine) (PS-*b*-P4VP) and 1-pyrenebutyric acid (PBA) in thin film for the first time. The supramolecular assembling of PS-*b*-P4VP and 1-pyrenebutyric acid changed the block copolymer morphology from cylindrical to lamella in thin film due to the increase of the volume fraction of P4VP (PBA). In both cases (parent block copolymer and SMA), the microdomains are oriented normal to the substrate after annealing in a selective solvent. Pure block copolymer shows cylindrical morphology with a periodicity ~26 nm, whereas the SMA shows lamellar morphology with a periodicity of ~29 nm. After fabricating the thin film from SMA, the major component 1-pyrenebutyric acid can be easily removed by dissolving the thin film in ethanol to transform the block copolymer thin film into nanotemplate or membrane. These nanotemplates were effectively used for the fabrication of arrays of nanowire of different functional material like metal or semiconductor. The block copolymer-based SMA thin film described here offers a simple root to fabricate block copolymer thin film with varying morphology from a single block copolymer composition. We believe that our study on block copolymer-based supramolecular assembly in thin film and the nanofabrication using these nanotemplates are considered to make a significant contribution in the development of nanoscience and nanotechnology.

**Acknowledgment.** B. K. Kuila and E. B. Gowd acknowledge financial support from the Alexander von Humboldt Foundation. This research was also supported by the priority program of Deutsche Forschungsgemeinschaft (SPP1165, Project No. STA324/31). We thank HASYLAB, DESY, Hamburg, Germany, for providing the facilities to use synchrotron radiation source for GISAXS experiments and BW4 beamline staff for the help in setting up the beamline at the HASYLAB.

## References and Notes

(1) Hamely, I. W. *The Physics of Block Copolymers*; Oxford University Press: New York, 1998.
(2) Bates, F. S.; Fredrickson, G. H. *Annu. Rev. Phys. Chem.* **1990**, *41*, 525.
(3) Krausch, G.; Magerle, R. *Adv. Mater.* **2002**, *14*, 1579.
(4) Bates, F. S.; Fredrickson, G. H. *Phys. Today* **1999**, *52*, 32.
(5) (a) Darling, S. B. *Prog. Polym. Sci.* **2007**, *32*, 1152. (b) Ramanathan, M.; Nettleton, E.; Darling, S. B. *Thin Solid Films* **2009**, *517*, 4474. (c) Knoll, A.; Horvat, A.; Lyakhova, K. S.; Krausch, G.; Sevink, G. J. A.; Zvelindovsky, A. V.; Magerle, R. *Phys. Rev. Lett.* **2002**, *89*, 035501.
(6) Chen, J. T.; Thomas, E. L.; Ober, C. K.; Mao, G. P. *Science* **1996**, *272*, 343.
(7) Thurn-Albrecht, T.; Schotter, J.; Kastle, G. A.; Emley, N.; Shibauchi, T.; Krusin-Elbaum, L.; Guarini, K.; Black, C. T.; Tuominen, M. T.; Russell, T. P. *Science* **2000**, *290*, 2126.
(8) Segalman, R. A. *Mater. Sci. Eng. R* **2005**, *48*, 191.
(9) Hawker, C. J.; Russell, T. P. *MRS Bull.* **2005**, *30*, 952.
(10) Morkved, T. L.; Lu, M.; Urbas, A. M.; Ehrichs, E. E.; Jaeger, H. M.; Mansky, P.; Russell, T. P. *Science* **1996**, *16*, 931.
(11) Mansky, P.; Chaikin, P. M.; Thomas, E. L. *J. Mater. Sci.* **1995**, *30*, 1987.
(12) Haberkorn, N.; Lechmann, M. C.; Sohn, B. H.; Char, K.; Gutmann, J. S.; Theato, P. *Macromol. Rapid Commun.* **2009**, *30*, 1146.
(13) Park, M.; Harrison, C.; Chaikin, P. M.; Register, R. A.; Adamson, D. H. *Science* **1997**, *276*, 1401.
(14) Lo, K.-H.; Chen, M.-C.; Ho, R.-M.; Sung, H.-W. *ACS Nano* **2009**, *3*, 2660.
(15) Rider, D. A.; Liu, K.; Eloi, J.-C.; Vanderark, L.; Yang, L.; Wang, J.-Y.; Grozea, D.; Lu, Z.-H.; Russell, T. P.; Manners, I. *ACS Nano* **2008**, *2*, 263.
(16) (a) Kuila, B. K.; Nandan, B.; Böhme, M.; Janke, A.; Stamm, M. *Chem. Commun.* **2009**, 5749. (b) Kuila, B. K.; Stamm, M. *J. Mater. Chem.* **2010**, 6086.
(17) Lee, J. I.; Cho, S. H.; Park, S.-M.; Kim, J. K.; Kim, J. K.; Yu, J.-W.; Kim, Y. C.; Russell, T. P. *Nano Lett.* **2008**, *8*, 2315.
(18) Valkama, S.; Ruotsalainen, T.; Nykanen, A.; Laiho, A.; Kosonen, H.; ten Brinke, G.; Ikkala, O.; Ruokolainen, J. *Macromolecules* **2006**, *39*, 9327.
(19) Ruokolainen, J.; Saariaho, M.; Ikkala, O.; ten Brinke, G.; Thomas, E. L.; Torkkeli, M.; Serimaa, R. *Macromolecules* **1999**, *32*, 1152.
(20) Ikkala, O.; ten Brinke, G. *Chem. Commun.* **2004**, 2131.
(21) Osuji, C. O.; Chao, C. Y.; Ober, C. K.; Thomas, E. L. *Macromolecules* **2006**, *39*, 3114.
(22) Sidorenko, A.; Tokarev, I.; Minko, S.; Stamm, M. *J. Am. Chem. Soc.* **2003**, *125*, 12211.
(23) van Zoelen, W.; Asumaa, T.; Ruokolainen, J.; Ikkala, O.; ten Brinke, G. *Macromolecules* **2008**, *41*, 3199.
(24) Tokarev, I.; Krenek, R.; Burkov, Y.; Schmeisser, D.; Sidorenko, A.; Minko, S.; Stamm, M. *Macromolecules.* **2005**, *38*, 507.
(25) (a) Laforgue, A.; Bazuin, C. G.; Prudhomme, R. E. *Macromolecules* **2006**, *39*, 6473. (b) Tang, C.; Lennon, E. M.; Fredrickson, G. H.; Kramer, E. J.; Hawker, C. J. *Science* **2008**, *322*, 429.
(26) Tung, S.-H.; Kalarickal, N. C.; Mays, J. W.; Xu, T. *Macromolecules* **2008**, *41*, 6453.
(27) (a) Kosonen, H.; Ruokolainen, J.; Knaapila, M.; Torkkeli, M.; Serimaa, R.; Bras, W.; Monkman, A. P.; ten Brinke, G.; Ikkala, O. *Synth. Met.* **2001**, *121*, 1277. (b) van Ekenstein, G. A.; Polushkin, E.; Nijland, H.; Ikkala, O.; ten Brinke, G. *Macromolecules* **2003**, *36*, 3684.
(28) Wood, K. C.; Little, S. R.; Langer, R.; Hammond, P. T. *Angew. Chem., Int. Ed.* **2005**, *44*, 6704.
(29) Faul, C. F. J.; Antonietti, M. *Adv. Mater.* **2003**, *15*, 673.
(30) Thunemann, A. F. *Prog. Polym. Sci.* **2002**, *27*, 1473.
(31) Valkama, S.; Lehtonen, O.; Lappalainen, K.; Kosenen, H.; Castro, P.; Repo, T.; Torkelli, M.; Serimaa, R.; ten Brinke, G.; Leskela, M.; Ikkala, O. *Macromol. Rapid Commun.* **2003**, *24*, 556.
(32) Ruokolainen, J.; Tanner, J.; ten Brinke, G.; Ikkala, O.; Torkelli, M.; Serimaa, R. *Macromolecules* **1995**, *28*, 7779.
(33) Ruokolainen, J.; Makinen, R.; Torkkeli, M.; Makela, T.; Serimaa, R.; ten Brike, G.; Ikkala, O. *Science* **1998**, *280*, 557.
(34) Ikkala, O.; ten Brinke, G. *Science* **2002**, *295*, 2407.
(35) Tung, S.-H.; Xu, T. *Macromolecules* **2009**, *42*, 5761.
(36) Krenek, R. PhD Thesis, Sächsische Landes- Staats- und Universitätsbibliothek (SLUB), Dresden, 2007.
(37) Chai, J.; Wang, D.; Fan, X.; Buriak, J. M. *Nature Nanotechnol.* **2007**, *2*, 500.
(38) Park, S.; Wang, J. Y.; Kim, B.; Xu, J.; Russell, T. P. *ACS Nano* **2008**, *2*, 766.
(39) Gowd, E. B.; Nandan, B.; Vyas, M. K.; Bigall, N. C.; Eychmüller, A.; Schlörb, H.; Stamm, M. *Nanotechnology* **2009**, *20*, 415302.
(40) Park, S.; Wang, J.-Y.; Kim, B.; Chen, W.; Russell, T. P. *Macromolecules* **2007**, *40*, 9059.
(41) Kim, G.; Libera, M. *Macromolecules* **1998**, *31*, 2569–2577.
(42) Kim, S. H.; Misner, M. J.; Xu, T.; Kimura, M.; Russell, T. P. *Adv. Mater.* **2004**, *16*, 226–231.
(43) Matsen, M. W.; Bates, F. S. *Macromolecules* **1996**, *29*, 1091.
(44) Alberda van Ekenstein, G. O. R.; Meyboom, R.; ten Brinke, G.; Ikkala, O. *Macromolecules* **2007**, *40*, 2109.

(45) van Zoelen, W.; Asumaa, T.; Ruokolainen, J.; Ikkala, O.; ten Brinke, G. *Macromolecules* **2008**, *41*, 3199.
(46) Zha, W.; Han, C. D.; Lee, D. H.; Han, S. H.; Kim, J. K.; Kang, J. H.; Park, C. *Macromolecules* **2007**, *40*, 2109.
(47) Gittins, D. I.; Caruso, F. *Angew. Chem., Int. Ed.* **2001**, *40*, 3001.
(48) Lo, K.-H.; Tseng, W.-H.; Ho, R.-M. *Macromolecules* **2007**, *40*, 2621.
(49) Jin, Y. H.; Kim, J. *Macromol. Res.* **2004**, *12*, 604.
(50) Ma, R. M.; Wei, X. L.; Dai, L.; Huo, H. B.; Qin, G. G. *Nanotechnology* **2007**, *18*, 205605.